

Carrier nonuniformity effects on the internal efficiency of multiquantum-well lasers

Joachim Piprek,^{a)} Patrick Abraham, and John E. Bowers

Electrical and Computer Engineering Department, University of California, Santa Barbara, California 93106

(Received 27 July 1998; accepted for publication 17 November 1998)

We investigate quantum efficiency limitations in InGaAsP/InP multiquantum-well (MQW) laser diodes emitting at 1.5 μm . At room temperature, the internal differential efficiency above threshold is found to be reduced mainly by increasing Auger recombination and spontaneous emission within the quantum wells. These carrier loss increments are commonly assumed negligible due to MQW carrier density clamping. Even with clamped average carrier density, increasing nonuniformity of the quantum well carrier population leads to enhanced losses. We analyze these loss enhancements using an advanced laser simulation software. Excellent agreement between measurements and simulations is obtained. © 1999 American Institute of Physics. [S0003-6951(99)02004-5]

The slope efficiency η_d is one of the most important performance parameters of laser diodes. It gives the percentage of electrons injected above threshold that contributes photons to the emitted laser beam. This efficiency $\eta_d = \eta_i \eta_o$ is restricted by carrier losses (η_i) and by photon losses (η_o). The internal efficiency η_i is equal to the fraction of current above threshold that results in stimulated emission of photons.¹ Carrier losses can be caused by spreading current (lateral carrier leakage; η_s), carrier escape from the active layers (vertical carrier leakage; η_e), and by recombination losses inside the active layers [Auger recombination, spontaneous emission, and Shockley–Read–Hall (SRH) recombination; η_r]. Thus, the internal efficiency is written as $\eta_i = \eta_s \eta_e \eta_r$.² All of these efficiencies are differential efficiencies describing the increment of losses above threshold.

In multiquantum-well (MQW) active regions, the carrier distribution between quantum wells is known to be nonuniform. This carrier nonuniformity has been investigated theoretically (see, e.g., Refs. 3 and 4) as well as by measurements on MQWs with nonuniform quantum wells.^{5–7} In InGaAsP/InP long-wavelength MQW lasers, the largest carrier density occurs in the quantum well closest to the p -doped side because electrons travel more easily across the MQW than holes.⁸ Long-wavelength lasers suffer from strong Auger recombination which rises proportional to the cube of the local carrier density. Thus, Auger recombination losses are expected to be highest in the p -side quantum well. Above threshold, the average MQW carrier density is clamped to the threshold level leading to the common assumption that MQW recombination losses remain constant ($\eta_r = 100\%$).¹ We will show that this assumption is not correct for multiquantum-well lasers. As the MQW carrier nonuniformity increases with rising current injection, the average MQW carrier density may remain constant, but the increment of Auger recombination within the more populated QWs is larger than its decrement within the less populated QWs.

We investigated the internal efficiency of InGaAsP/InP

broad-area ($W = 50 \mu\text{m}$) in-plane lasers emitting at 1.5 μm wavelength. The active region of the laser structure consists of six 6.5-nm-wide 1% compressively strained QWs. The barriers are 5.5 nm thick and are made of lattice matched InGaAsP (1.25 μm band gap wavelength). The MQW is sandwiched between 100 nm undoped InGaAsP (1.15 μm) separate confinement layers (SCLs). The band diagram of our laser is given in Fig. 1.

Typical results of pulsed lasing power versus current (PI) measurements are shown in Fig. 2 (dots) for different laser lengths L . The change of the PI slope efficiency η_d with laser length is used to extract the internal efficiency η_i .¹ The slopes from Fig. 2 lead to $\eta_i = (92 \pm 3)\%$ indicating about 8% carrier loss. Since lateral leakage is negligible in broad area lasers ($\eta_s \approx 100\%$) and η_r was first assumed to be 100%, the measured carrier losses were attributed to vertical leakage (η_e).

To restrict vertical leakage currents which use to escalate at higher temperatures, a second laser structure was fabricated which contains an additional strained $\text{In}_{0.81}\text{Ga}_{0.19}\text{P}$ electron stopper layer between SCL and p -InP.⁹ The stopper layer has a conduction band offset to InP of $\Delta E_c \approx 50 \text{ meV}$ but it does not hinder hole transport due to the smaller light-

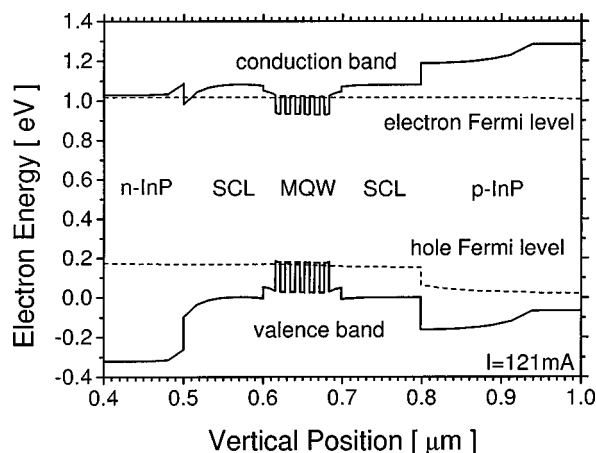


FIG. 1. Energy band diagram of our laser at threshold including quasi-Fermi levels (dashed).

^{a)}Electronic mail: piprek@ece.ucsb.edu

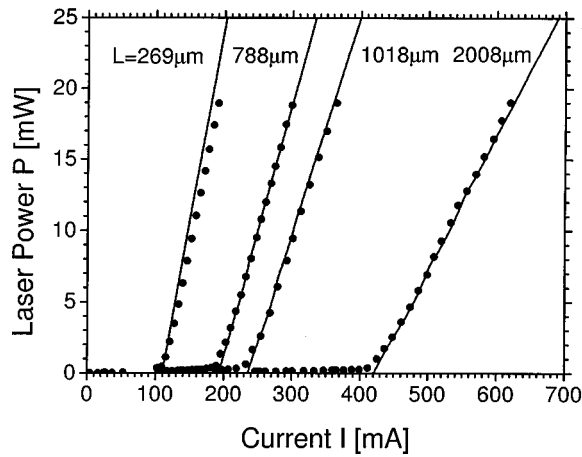


FIG. 2. Pulsed light power vs current characteristics (0.05% duty cycle) at different laser length L (dots—measurement, lines—simulation).

hole band gap. This InGaP layer was expected to reduce electron leakage from the active region but no significant change in the laser characteristics is measured at room temperature indicating negligible leaking.⁹ Since both η_e and η_s seem to be close to 100% in our lasers, these experimental results direct our attention towards recombination losses (η_r) to account for the reduced internal efficiency measured.

In the following, we analyze carrier losses at room temperature using an advanced laser simulation tool.^{10,11} The software calculates the optical gain in strained quantum wells based on the **kp** method including valence band mixing and carrier-carrier interaction. The computed photoluminescence spectrum as well as the emission wavelength are in good agreement with our measurements. The current calculation is based on a drift-diffusion model including thermionic emission at heterointerfaces.¹² The band offset ratio is $\Delta E_c/\Delta E_{\text{gap}}=0.36$. The measured internal absorption $\alpha_i=18\text{ cm}^{-1}$ is used for long lasers. With shorter lasers, the threshold carrier density rises slightly and so does the internal absorption. Excellent agreement with the PI measurements in Fig. 2 is obtained (lines) assuming an average facet power reflectivity of $R=0.28$. The shortest laser is selected for further analysis.

Electron leakage from the active region can be identified as minority carrier current in the p -InP cladding layer. At threshold ($I_{\text{th}}=110\text{ mA}$), only 0.3% of the *total* electron current leaks into the p cladding, i.e., adding an InGaP barrier cannot have any significant effect at room temperature. Hole leakage is even smaller. Figure 3 shows the increase of the vertical leakage current above threshold. At 20 mW output power ($I=180\text{ mA}$), the leakage current increment above threshold ΔI_e contributes 1% to the total current increment $\Delta I=I-I_{\text{th}}$ resulting in $\eta_e=1-\Delta I_e/\Delta I=99\%$. At very high injection ($I=323\text{ mA}$), the leakage losses amount to 3.4% (Fig. 3). This electron leakage is correlated to the increasing nonuniformity of the quantum-well electron population which leads to enhanced electron overflow into the p -side SCL (Fig. 4). The electron density ratio between the p -side QW and the n -side QW rises from 1.08 (121 mA) to 1.21 (323 mA). Holes exhibit a very similar nonuniformity. The average MQW electron density increases by a small factor of 1.015 which is mainly due to the nonlinear gain versus car-

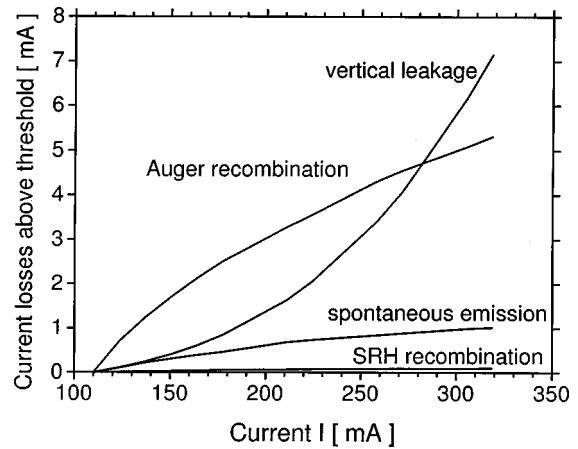


FIG. 3. Computed increase of current losses above threshold ($L=269\text{ }\mu\text{m}$).

rier density relation. However, the calculated leakage carrier losses are too small to account for the measured carrier losses of 8%.

Carrier losses due to Auger recombination, spontaneous emission, and SRH recombination are analyzed by integrating the recombination rates at different bias points. Typical recombination parameters are used in the model ($C=10^{-28}\text{ cm}^6\text{ s}^{-1}$, $B=10^{-10}\text{ cm}^3\text{ s}^{-1}$, and $A=10^8\text{ s}^{-1}$, resp.)¹³ as confirmed by a previous analysis of laser measurements.¹⁴ At threshold, 66% of the *total* current feeds Auger recombination, 30% spontaneous emission, and 4% SRH recombination. Above threshold, those carrier losses continue to grow (Fig. 3) which is largely due to the increasing nonuniformity of the MQW carrier distribution (Fig. 4). SRH recombination grows linear with the local carrier density and it reflects only the change in average carrier density. Spontaneous emission and Auger recombination exhibit a superlinear dependence on the local carrier density and increasing carrier nonuniformity (Fig. 4) causes stronger *total* recombination losses (Fig. 5) even if the average carrier density remains constant. The increment in total Auger recombination is sublinear in Fig. 3 since an increasing percentage of the total current is consumed by vertical leakage. Adding all current losses in Fig. 3 to ΔI_{loss} leads to the internal efficiency $\eta_i=1-\Delta I_{\text{loss}}/\Delta I$. At $P=20\text{ mW}$ ($I=180\text{ mA}$), we obtain $\eta_i=94\%$ which is in

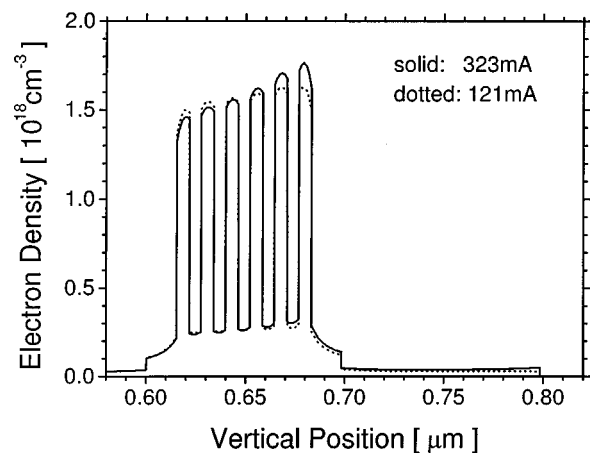


FIG. 4. Electron distribution as calculated for low (dotted line) and for high (solid line) injection current ($L=269\text{ }\mu\text{m}$).

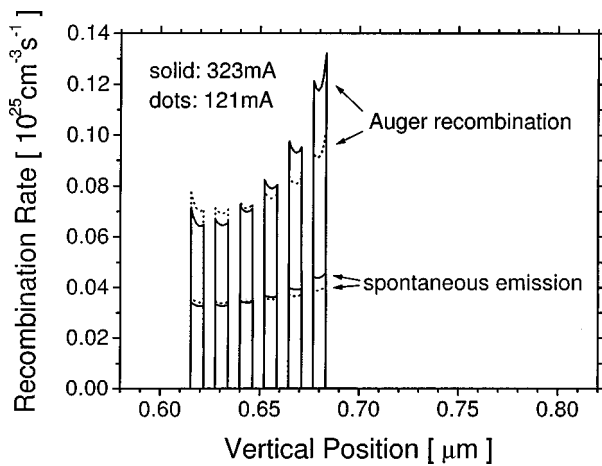


FIG. 5. Auger recombination and spontaneous emission within each of the six quantum wells as calculated for low (dotted line) and for high (solid line) injection current ($L=269 \mu\text{m}$).

excellent agreement with our experimental results from Fig. 2. With $\eta_e=99\%$ and $\eta_s=100\%$, a recombination related efficiency of $\eta_r=95\%$ is deduced for our lasers. These results slightly depend on the injection current. At very high injection ($I=323 \text{ mA}$), we obtain $\eta_e=97\%$, $\eta_r=96\%$, and $\eta_i=93\%$ from Fig. 3.

In conclusion, the nonuniformity of the carrier distribution in multi-quantum well active regions is found to enhance carrier losses and to reduce the internal quantum efficiency

of laser diodes. Contrary to a common assumption, a major increment of carrier losses above threshold is caused by Auger recombination and by spontaneous emission within the quantum wells of our lasers. At room temperature, we observe only a minor contribution from electron leakage. An analysis of high-temperature effects will be published elsewhere.

¹L. A. Coldren and S. W. Corzine, *Diode Lasers and Photonic Integrated Circuits* (Wiley, New York, 1995).

²P. M. Smowton and P. Blood, *IEEE J. Sel. Top. Quantum Electron.* **3**, 491 (1997).

³N. Tessler and G. Eisenstein, *Appl. Phys. Lett.* **62**, 10 (1993).

⁴M. Grupen and K. Hess, *IEEE J. Quantum Electron.* **34**, 120 (1998).

⁵K. Frojdh, S. Marcinkevicius, U. Olin, C. Silfvenius, B. Stalacke, and G. Landgren, *Appl. Phys. Lett.* **69**, 3695 (1996)

⁶H. Yamazaki, A. Tomita, M. Yamaguchi, and Y. Sasaki, *Appl. Phys. Lett.* **71**, 767 (1997).

⁷B.-L. Lee and C.-F. Lin, *Conf. On Lasers and Electro-Optics CLEO, CWF17, San Francisco, 1998* (unpublished).

⁸M. Hybertsen, M. A. Alam, R. K. Smith, G. A. Barraff, and M. R. Pinto, *24th International Symposium on Compound Semiconductors, TuF1, San Diego 1997* (unpublished).

⁹P. Abraham, J. Piprek, S. DenBaars, and J. Bowers, *International Conference on InP and Related Materials IPRM, ThP-51, Tsukuba, 1998* (unpublished).

¹⁰PICS3D by Crosslight Software, Inc.

¹¹Z.-M. Li, *Proc. SPIE* **2994**, 698 (1997).

¹²S. M. Sze, *Physics of Semiconductor Devices* (Wiley, New York, 1981).

¹³G. P. Agrawal and N. K. Dutta, *Semiconductor Lasers* (Van Nostrand Reinhold, New York, 1993).

¹⁴J. Piprek, D. Babic, and J. E. Bowers, *J. Appl. Phys.* **81**, 3382 (1997).